

Equilibrium and non-equilibrium fluctuations in a glass-forming liquid

Azita Parsaeian and Horacio E. Castillo

Department of Physics and Astronomy, Ohio University, Athens, OH, 45701, USA

(Dated: November 17, 2008)

Glass-forming liquids display strong fluctuations – dynamical heterogeneities – near their glass transition. By numerically simulating a binary Weeks-Chandler-Andersen liquid and varying both temperature and timescale, we investigate the probability distributions of two kinds of local fluctuations in the non-equilibrium (aging) regime and in the equilibrium regime; and find them to be very similar in the two regimes and across temperatures. We also observe that, when appropriately rescaled, the integrated dynamic susceptibility is very weakly dependent on temperature and very similar in both regimes.

PACS numbers: 64.70.Q-, 61.20.Lc, 61.43.Fs, 05.40.-a

Keywords: glass-forming liquids, spatially heterogeneous dynamics, relaxation, aging, nonequilibrium dynamics, Lennard-Jones mixture, Weeks-Chandler-Andersen potential, supercooled liquid, molecular dynamics, fluctuation phenomena, noise.

The study of fluctuations in statistical mechanics has had a long history, starting from Einstein’s seminal work on Brownian motion. Recent research on fluctuations has focused on nonequilibrium problems, such as turbulence [1], non-equilibrium steady state phenomena [2], single molecule experiments in biophysics [3], or the relaxation of large perturbations [4]. In the present work, we want to use glasses as a convenient laboratory to study fluctuations in both equilibrium and out of equilibrium states; *i.e.* on both sides of the (kinetic) glass “transition”.

As experimentally observed, the glass transition is not a sharp thermodynamic phase transition [5], but rather a dynamical crossover. As the system approaches this crossover, the equilibration time τ_{eq} gradually increases, until it eventually becomes longer than the representative laboratory timescale t_{lab} [6, 7]. Beyond the glass transition, the system cannot equilibrate in laboratory timescales. This leads to the emergence of new phenomena, such as physical aging, *i.e.* the breakdown of time translation invariance (TTI). Besides the slowdown of the dynamics, also dynamical heterogeneities [7, 8], *i.e.* strong local fluctuations in the properties of glass-forming liquids, are observed both in the equilibrium regime [9, 10, 11] and in the aging regime [12, 13, 14, 15, 16, 17]. It is not clear, though, to what degree the properties of those fluctuations depend on whether they are observed in one or the other regime. In the present work, we address this question in the context of a detailed molecular dynamics simulation of a simple glass model probing the aging regime, the equilibrium regime, and the crossover regime between the two.

A theoretical framework based on the presence of a Goldstone mode in the aging dynamics [18] that gives rise to local fluctuations in the age of the sample [19, 23] predicts that probability distributions of local fluctuations in the aging regime are approximately independent of the waiting time t_w at fixed values of the two-time global correlation $C_{\text{global}}(t, t_w)$. This prediction, initially proposed for spin glasses [19], has been found to apply also to off-

lattice models of aging structural glasses [15, 17] (where C_{global} is the self part of the intermediate scattering function: $C_{\text{global}}(t, t_w) \equiv \frac{1}{N} \sum_{j=1}^N \exp(i\mathbf{q} \cdot (\mathbf{r}_j(t) - \mathbf{r}_j(t_w)))$). Additionally, it has been found that the dynamic spatial correlations in an aging structural glass display a simple scaling behavior as a function of C_{global} [16, 17]. In what follows we address the question of whether these same scaling behaviors extend to the equilibrium regime of an off-lattice structural glass model.

In order to observe both equilibrium and aging phenomena, one could either reduce the temperature T of the thermal reservoir that the system is coupled to beyond the glass transition temperature T_g at a fixed laboratory timescale t_{lab} , or reduce t_{lab} until it becomes shorter than τ_{eq} , at fixed reservoir temperature T . Here we use both approaches. To observe genuinely glassy dynamics, we make sure that T is low enough that two-step relaxation is observed, and that timescales are much longer than the timescale of the first step.

We simulate a 80 : 20 binary mixture of particles of mass $M_A = M_B = M$, in three dimensions, at a number density $\rho = 1.204$, interacting via short-range, purely repulsive Weeks-Chandler-Andersen (WCA) potentials [20]: $V_{\alpha,\beta} = 4\epsilon_{\alpha,\beta} \left[\left(\frac{\sigma_{\alpha,\beta}}{r} \right)^{12} - \left(\frac{\sigma_{\alpha,\beta}}{r} \right)^6 + 1 \right] \theta(r_{\alpha,\beta}^{\text{cutoff}} - r)$, where $\alpha, \beta \in \{A, B\}$ denotes the particle type, $\epsilon_{\alpha,\beta}$ and $\sigma_{\alpha,\beta}$ are taken as in [21, 22], $\theta(x)$ is the Heaviside theta function, and $r_{\alpha,\beta}^{\text{cutoff}} \equiv 2^{1/6} \sigma_{\alpha,\beta} \approx 1.1225 \sigma_{\alpha,\beta}$ makes $V(r)$ and $\partial V / \partial r$ continuous for all $r > 0$. We take $k_B = 1.0$, and the units of length, energy and time as σ_{AA} , ϵ_{AA} and $\tau_{LJ} \equiv (\sigma_{AA}^2 M / 48 \epsilon_{AA})^{1/2}$ respectively, where τ_{LJ} represents roughly the timescale for vibrational motion in the system. Initially the system is equilibrated at a high temperature: $T_i = 5.0$, and then instantaneously quenched to a final temperature $T_f \ll T_i$. The top panel of Fig. 1 illustrates the temperature and time regimes for which we show results. We take three different T_f ’s. For $T_f = 0.236 \approx 0.9 T_{\text{MCT}}$, only the aging regime is observed within our simulation time frame.

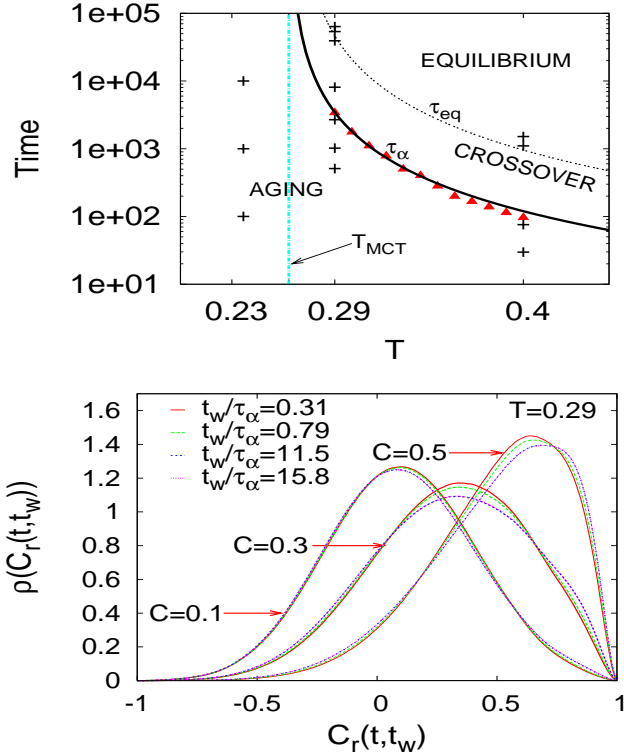


FIG. 1: *Top panel:* Timescales as functions of the temperature. “+” symbols: (temperature, waiting time) pairs for which we show our results. Triangles: α relaxation times for $T = 0.29, \dots, 0.40$. Full line: fit of τ_α to $\tau_\alpha = a(T - T_{\text{MCT}})^{-\gamma}$. Dotted line: τ_{eq} , estimated as $\tau_{\text{eq}} \sim 10\tau_\alpha$ (see text). Vertical dash-dotted line: T_{MCT} . *Bottom panel:* Probability distribution $\rho(C_r)$ at $T = 0.29$, when $C_{\text{global}}(t, t_w) = 0.1, 0.3, 0.5$, for $t_w/\tau_\alpha = 0.31, 0.79$ (aging) and $t_w/\tau_\alpha = 11.5, 15.8$ (equilibrium). The two equilibrium plots overlap perfectly. The coarse graining region contains on average 6.6 particles.

For $T_f = 0.29 \approx 1.1T_{\text{MCT}}$ and $T_f = 0.4 \approx 1.5T_{\text{MCT}}$, we observe both the aging and equilibrium regimes. Here, T_{MCT} denotes the Mode Coupling Theory (MCT) critical temperature. We define τ_α by the condition $\lim_{t_w \rightarrow \infty} C(t_w + \tau_\alpha, t_w) = 1/e$ and find it for the temperatures $T = 0.29, 0.30 \dots 0.4$. We observe that for $2.9 \leq T \leq 3.4$, the equilibrium $C(t, t_w)$ displays two step relaxation and also scaling behavior as predicted by MCT. Following [22], we fit $\tau_\alpha = (T - T_{\text{MCT}})^{-\gamma}$ in that range, and find $T_{\text{MCT}} = 0.263 \pm 0.01$ and $\gamma = 2.1 \pm 0.7$.

The time of the quench is taken as the origin of times $t = 0$. In our simulations, t_{lab} is replaced by t_w . We find that aging effects are strongest for $t_w/\tau_\alpha \lesssim 2$. For $2 \lesssim t_w/\tau_\alpha \lesssim 10$ the aging effects gradually become weaker with increasing t_w until they disappear for $t_w/\tau_\alpha \sim 10$. We thus estimate $\tau_{\text{eq}} \sim 10\tau_\alpha$. We show results for a 1,000 particle system, with 5000, 9000 and 10,000 independent thermal histories when $T_f = 0.236$, $T_f = 0.29$, and $T_f = 0.4$ respectively.

We present results for the probability distribu-

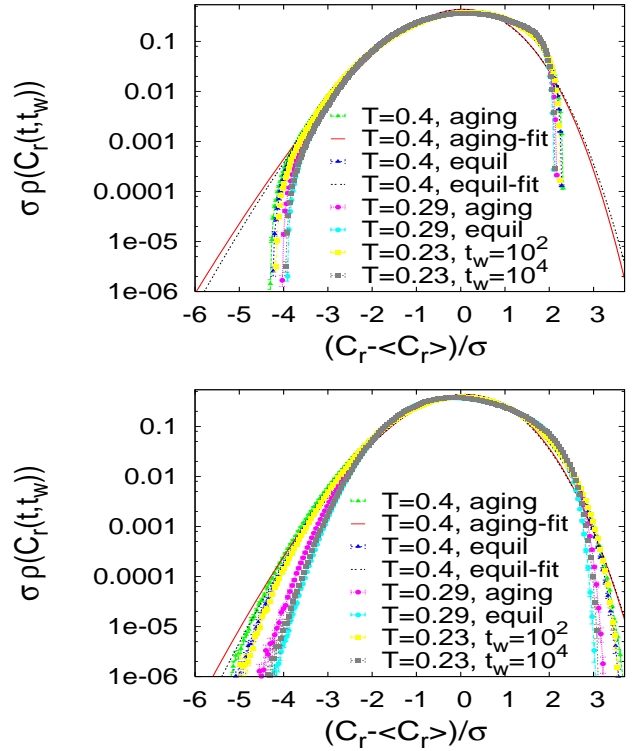


FIG. 2: Rescaled probability distributions $\sigma_C \rho(C_r)$ as functions of the normalized fluctuation $(C_r - C_{\text{global}})/\sigma_C$ in the two-time correlation, shown at $t_w/\tau_\alpha = 0.79$ (aging regime) and $t_w/\tau_\alpha = 11.5$ (equilibrium regime), for temperatures $T = 0.4$ (triangles), $T = 0.29$ (circles) and $T = 0.236$ (squares), with $C_{\text{global}}(t, t_w) = 0.3$. Generalized Gumbel fits to the distributions for $T = 0.4$ are shown with thin lines. *Top panel:* Coarse graining region containing on average 6.6 particles/box. *Bottom panel:* Coarse graining region containing on average 30.5 particles/box.

tions of observables which probe local fluctuations in small regions of the system: the local coarse grained two-time correlation function [15] $C_r(t, t_w) \equiv \frac{1}{N(B_r)} \sum_{\mathbf{r}_j(t_w) \in B_r} \cos(\mathbf{q} \cdot (\mathbf{r}_j(t) - \mathbf{r}_j(t_w)))$, and the particle displacements $\Delta x_j(t, t_w) = x_j(t) - x_j(t_w)$ along one direction [10, 15, 24]. Here B_r represents a small coarse graining box around the point \mathbf{r} in the system and $N(B_r)$ is the number of particles present at the waiting time t_w in the box B_r . We choose a value of q that corresponds to the main peak in the structure factor $S(q)$ of the system, $q = 7.2$. In order to probe the spatial correlations of the fluctuations, we also consider the generalized 4-point density susceptibility $\chi_4 \equiv \int d^3\mathbf{r} g_4(\mathbf{r}, t, t_w)$ [11, 16, 25], where $g_4(\mathbf{r}, t, t_w)$ is a 4-point (2-time, 2-position) correlation function [11, 16].

In the bottom panel of Fig. 1 we show the probability distributions $\rho(C_r)$ for $C_{\text{global}}(t, t_w) = 0.1, 0.3, 0.5$. We observe that, for fixed value of $C_{\text{global}}(t, t_w)$, the probability distributions are approximately invariant between the two regimes. These results extend those found for the

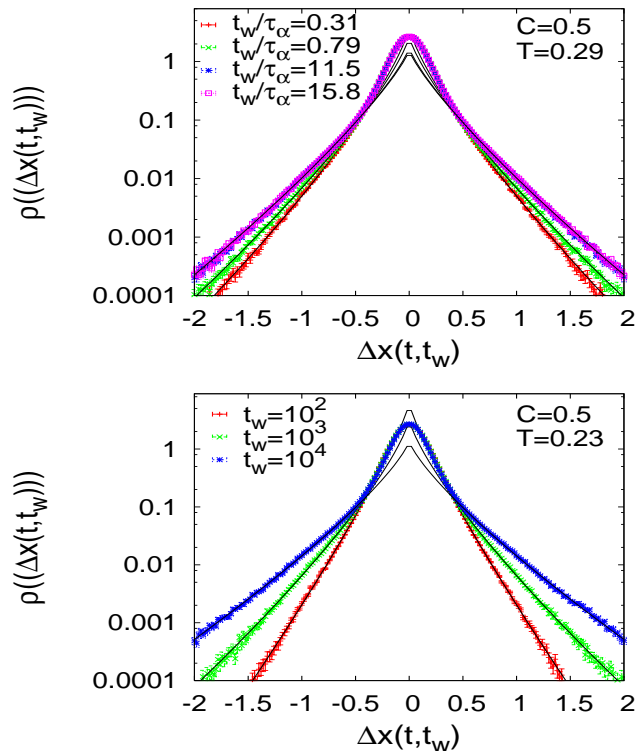


FIG. 3: $\rho(\Delta x)$ for $C_{\text{global}}(t, t_w) = 0.5$, plotted with a logarithmic vertical axis to emphasize the tails of the distributions. Fits to the tails by a nonlinear exponential form are shown with full lines. *Top panel:* $T = 0.29$. $t_w = 0.31\tau_\alpha, 0.79\tau_\alpha$ are in the aging regime; whilst $t_w = 11.5\tau_\alpha, 15.8\tau_\alpha$, which give perfectly overlapping results, are in the equilibrium regime. *Bottom Panel:* $T = 0.23$. Only the aging regime is accessible; $t_w = 10^2, 10^3, 10^4$.

aging regime of a binary Lennard-Jones (LJ) glass [15].

Fig. 2 shows the rescaled probability distributions $\sigma_C \rho(C_r)$ versus the normalized fluctuation $(C_r - C_{\text{global}})/\sigma_C$ in the one-point two-time correlator, for coarse graining regions of two sizes, for the temperatures $T = 0.23$, $T = 0.29$ and $T = 0.4$. We observe a very good collapse of the data for different t_w and different temperatures for the smaller coarse graining size, and a slightly less good collapse for the larger coarse graining size. This suggests that the weak dependence on t_w may be due to the time dependence of the dynamic correlation length [15]. In [23] it has been argued that the probability distribution of the normalized fluctuations $(C_r - C_{\text{global}})/\sigma_C$ can be described well by a generalized Gumbel distribution Φ_{Gumbel} [1]. Fig. 2 shows that fits of our data to Φ_{Gumbel} become better for a larger coarse graining region, i.e. when averaging affects have started to modify the distribution [1].

In Fig. 3 we show the probability distribution $\rho(\Delta x)$ of the particle displacements, with $C_{\text{global}}(t, t_w) = 0.5$, for both $T_f = 0.29 > T_{\text{MCT}}$ (top panel) and $T_f = 0.23 < T_{\text{MCT}}$ (bottom panel). We use semilog plots to emphasize

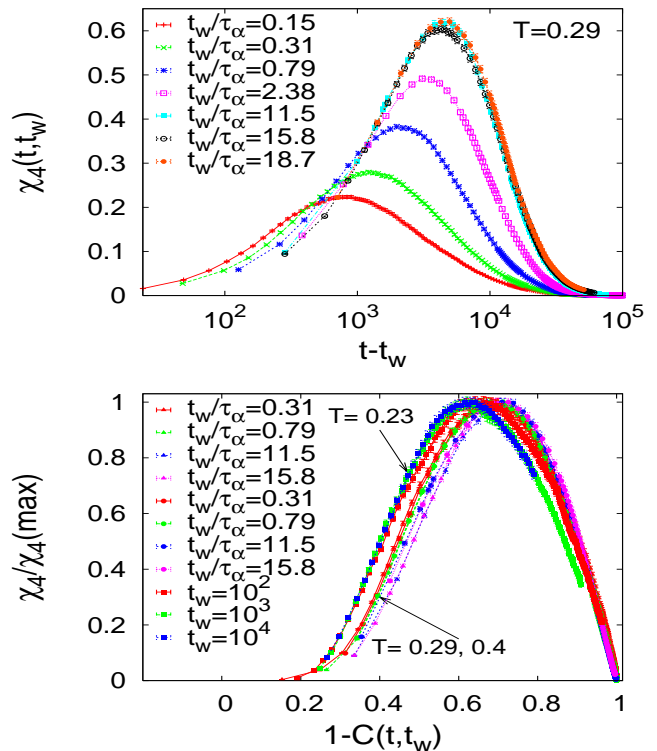


FIG. 4: *Top panel:* $\chi_4(t, t_w)$ as a function of $t - t_w$ for $T = 0.29$. *Bottom panel:* χ_4 divided by its maximum value $\chi_4(\text{max})$, plotted as a function of $1 - C$, with $C \equiv C_{\text{global}}(t, t_w)$ for $T = 0.4$ (triangles), $T = 0.29$ (circles) and $T = 0.23$ (squares).

the tails of the distributions. The distributions are very similar to those determined by confocal microscopy for an equilibrium sterically stabilized colloidal liquid near its glass transition [10], and also to the ones found in simulations of an aging binary LJ glass [15]; but markedly different from those found by confocal microscopy in an attracting colloid [24]. For small to moderate values of Δx , the data for different t_w and temperatures collapse very well with each other and with a common gaussian fit, as long as C_{global} is constant (not shown). We find, however, that for fixed $C_{\text{global}}(t, t_w)$, the tails of the distribution become wider for increasing t_w . The tails can be fit in the region $|\Delta x| > 0.5$ by a nonlinear exponential form $\rho(\Delta x) \approx N \exp(-|\Delta x/a|^\beta)$, with $\beta \sim 1$ decreasing monotonically with increased t_w [15]. For the case of $T > T_{\text{MCT}}$ both the tails and the value of β gradually saturate as the system approaches equilibrium.

To quantify the spatial correlation of dynamical fluctuations, the 4-point density susceptibility $\chi_4(t, t_w)$ [11, 16, 25] and similar quantities have been used both in numerical simulations [11, 16, 25] and in experiments [26, 27, 28, 29]. The top panel of Fig. 4 shows $\chi_4(t, t_w)$ as a function of $t - t_w$ at $T_f = 0.29$, for various t_w . We have found that $\chi_4(t, t_w)$ has a peak whose

height and location grow with t_w as long as the system is aging. This behavior as t_w is increased is observed experimentally in a coarsening foam [26], and analogous to the behavior of supercooled liquids as the temperature is reduced [27] and of granular systems as the area fraction is increased [28]. In the bottom panel of Fig. 4 we test for a possible scaling behavior with $C \equiv C_{\text{global}}$, by plotting the rescaled quantity $\chi_4/\chi_4(\text{max})$ as a function of $1 - C$, for $T_f = 0.23, 0.29, 0.4$. An exact collapse would implicate the factorization $\chi_4(t, t_w) = \chi_4^\circ(t_w)\phi(C(t, t_w))$, where $\chi_4^\circ(t_w) \equiv \chi_4(t, t_w)|_{C(t, t_w)=1/e}$ is a rescaling factor that depends only on t_w until it saturates when the system equilibrates; and $\phi(C(t, t_w))$ is a scaling function which depends on times only through the value of the intermediate scattering function $C(t, t_w)$. We observe that the curves approximately collapse into two groups, one for $T > T_{\text{MCT}}$ and another for $T < T_{\text{MCT}}$, with a slight horizontal shift between the two groups. Curves for the same temperature approximately collapse, although a slight systematic variation with t_w remains.

In summary, we have analyzed the probability distributions of local two-time observables and the spatial correlations of fluctuations in the equilibrium and aging regimes in a simple glass model. We do find some differences between the two regimes. For example, the tails of the probability distributions of one-particle displacements $\rho(\Delta x)$ become slightly wider as t_w grows at constant $C_{\text{global}}(t, t_w)$. Also, the rescaled generalized susceptibility $\chi_4/\chi_4(\text{max})$, when plotted as a function of $1 - C_{\text{global}}$, shows slight systematic dependences on t_w and on T . However, those differences are minor, and

the similarities are quite striking. In general terms, the simple scaling behaviors previously observed in the aging regime [15, 16] extend to the equilibrium regime. On one hand, both the probability distributions of local two-time correlations and the probability distributions of one-particle displacements are approximately invariant between the two regimes as long as the total correlation $C_{\text{global}}(t, t_w)$ is kept constant. On the other hand, the rescaled dynamic susceptibility $\chi_4/\chi_4(\text{max})$, when plotted against $1 - C_{\text{global}}(t, t_w)$, is also approximately invariant between the two regimes. Additionally, we find that the probability distributions $\rho(C_r)$ of local two-time correlations can be fitted by generalized Gumbel forms [1, 23], as long as the coarse graining size is relatively large. Finally, the scaling functions describing the distribution of local two-time correlations and the dynamic susceptibilities are very weakly dependent on temperature across the range from $T \lesssim T_{\text{MCT}}$ to $T > T_{\text{MCT}}$, and qualitatively similar to those found in an aging LJ glass [15, 16].

H. E. C. thanks L. Berthier, J. P. Bouchaud, L. Cugliandolo, S. Glotzer, N. Israeloff, M. Kennett, M. Kilfoil, D. Reichman, E. Weeks, and particularly C. Chamon for suggestions and discussions. This work was supported in part by DOE under grant DE-FG02-06ER46300, by NSF under grant PHY99-07949, and by Ohio University. Numerical simulations were carried out at the Ohio Supercomputing Center. H. E. C. acknowledges the hospitality of the Aspen Center for Physics, where part of this work was performed.

-
- [1] S. T. Bramwell, P. C. W. Holdsworth and J.F. Pinton, *Nature* **396** 552 (1998); S. T. Bramwell, K. Christensen, J.-Y. Fortin, P. C. W. Holdsworth, H. J. Jensen, S. Lise, J. M. López, M. Nicodemi, J.-F. Pinton, and M. Sellitto, *Phys. Rev. Lett.* **84**, 3744 (2000).
- [2] T. Taniguchi and E. G. D. Cohen, *J. Stat. Phys.* **130** 633 (2008).
- [3] F. Ritort, *C. R. Physique* **8** 528 (2007).
- [4] G. Boffetta, G. Lacorata, S. Musacchio, and A. Vulpiani, *Chaos*, **13** 806 (2003).
- [5] However, such transition may exist at a lower temperature [6].
- [6] R. Zallen, *The Physics of Amorphous Solids*, (John Wiley, New York, 1983); E. Donth, *The Glass Transition*, (Springer-Verlag, Berlin, 2001); P. G. Debenedetti F. H. Stillinger, *Nature* **410**, 259 (2001).
- [7] M. D. Ediger, *Annu. Rev. Phys. Chem.* **51**, 99 (2000).
- [8] H. Sillescu, *J. Non-Crystal. Solids* **243**, 81 (1999).
- [9] Kegel, W. K., and Blaaderen, A. V. *Science* **287**, 290 (2000).
- [10] E. R. Weeks, J. C. Crocker, A. C. Levitt, A. Schofield, and D. A. Weitz, *Science* **287**, 627 (2000); E. R. Weeks and D. A. Weitz, *Phys. Rev. Lett.* **89**, 095704 (2002).
- [11] C. Donati, S. C. Glotzer, P. H. Poole, *Phys. Rev. Lett.* **82**, 5064 (1999); W. Kob, C. Donati, S. J. Plimpton, P. H. Poole, and S. C. Glotzer, *Phys. Rev. Lett.* **79**, 2827 (1997); Glotzer, S. C., *J. Non-Crystal. Solids* **274**, 342 (2000); N. Lacevic, F. W. Starr, T. B. Schroder and S. C. Glotzer, *J. Chem. Phys.* **119**, 7372 (2003).
- [12] R. E. Courtnall and E. R. Weeks, *J Phys C* **15**, S359 (2003).
- [13] Sinnathamby, K. S., Oukris, H., and Israeloff, N. E., *Phys. Rev. Lett.* **95**, 067205 (2005).
- [14] G. Parisi, *J. Phys. Chem. B* **103** 4128-4131 (1999)
- [15] H. E. Castillo and A. Parsaeian, *Nat. Phys.* **3**, 26 (2007).
- [16] Azita Parsaeian and Horacio E. Castillo, *arXiv:cond-mat/0610789*.
- [17] Azita Parsaeian and Horacio E. Castillo, *submitted*.
- [18] C. Chamon, M. P. Kennett, H. E. Castillo, and L. F. Cugliandolo, *Phys. Rev. Lett.* **89**, 217201 (2002); H. E. Castillo, *Phys. Rev. B*, *in press*, *arXiv:0801.0014*.
- [19] H. E. Castillo, C. Chamon, L. F. Cugliandolo, and M. P. Kennett, *Phys. Rev. Lett.* **88**, 237201 (2002); H. E. Castillo, C. Chamon, L. F. Cugliandolo, J. L. Iguain, and M. P. Kennett, *Phys. Rev. B* **68**, 134442 (2003).
- [20] Chandler. D, Weeks J. D., Andersen H. C., *Science* **220**, 787 (1983).
- [21] W. Kob and J. L. Barrat, *Phys. Rev. Lett.* **78**, 4581 (1997).
- [22] W. Kob, H. C. Andersen. *Phys. Rev. Lett.* **73**, 1376 (1994).

- [23] C. Chamon, P. Charbonneau, L. F. Cugliandolo, D. R. Reichman, and M. Sellitto, *J. Chem. Phys.* **121**, 10120 (2004).
- [24] P. Chaudhuri, Y. Gao, L. Berthier, M. Kilfoil, W. Kob, [arXiv:0712.0887](https://arxiv.org/abs/0712.0887).
- [25] C. Toninelli, M. Wyart, L. Berthier, G. Biroli, J. P. Bouchaud, *Phys. Rev. E* **71**, 041505 (2005)
- [26] P. Mayer *et al.*, *Phys. Rev. Lett.* **93**, 115701 (2004).
- [27] L. Berthier *et al.*, *Science* **310**, 1797, (2005);
- [28] O. Dauchot, G. Marty and G. Biroli, *Phys. Rev. Lett.* **95**, 265701 (2005); A. R. Abate and D. J. Durian, *Phys. Rev. E* **76**, 021306 (2007); A. S. Keys, A. R. Abate, S. C. Glotzer, and D. J. Durian, *Nature Physics* **3**, 260 (2007).
- [29] A. Duri and L. Cipelletti, *Europhys. Lett.*, **76**, 972 (2006).